

# Affordance detection with Dynamic-Tree Capsule Networks

A. Rodríguez-Sánchez<sup>1</sup> S. Haller-Seeber<sup>1</sup> D. Peer<sup>1</sup> C. Engelhardt<sup>1</sup> J. Mittelberger<sup>1</sup> M. Saveriano<sup>2</sup>

**Abstract**—Affordance detection from visual input is a fundamental step in autonomous robotic manipulation. Existing solutions to the problem of affordance detection rely on convolutional neural networks. However, these networks do not consider the spatial arrangement of the input data and miss parts-to-whole relationships. Therefore, they fall short when confronted with novel, previously unseen object instances or new viewpoints. One solution to overcome such limitations can be to resort to capsule networks. In this paper, we introduce the first affordance detection network based on dynamic tree-structured capsules for sparse 3D point clouds. We show that our capsule-based network outperforms current state-of-the-art models on viewpoint invariance and parts-segmentation of new object instances through a novel dataset we only used for evaluation and it is publicly available from [github.com/gipfelen/DTCG-Net](https://github.com/gipfelen/DTCG-Net). In the experimental evaluation we will show that our algorithm is superior to current affordance detection methods when faced with grasping previously unseen objects thanks to our Capsule Network enforcing a parts-to-whole representation.

## I. INTRODUCTION

3D sensing is essential in robotics and is one of the major research areas in the field. Thanks to the recent advances of deep learning, much progress has been achieved in many challenging tasks like object classification or affordance detection [1], [2]. Existing approaches typically rely on convolutional neural networks (CNN) due to their outstanding performance in most vision applications. However, CNN-based networks consider the spatial arrangement the input data only based on local proximity and not in terms of the arrangement of constituent parts as they do not explicitly encode parts-to-whole relationships. The consequence of this limitation is a drop in performance when faced with new object instances or new viewpoints.

An evolution of CNNs are Capsule Networks that group multiple neurons into a single Capsule which are layer-wise connected through a special routing-procedure [3]. Recently, Capsule Networks have been successfully applied to 3D data [4] for tasks like reconstruction, segmentation, and interpolation. Goyal et al. [5] already motivated that additional inductive biases should be added to deep learning methods in order to go from a reasonably good *in-distribution generalization* in highly supervised learning tasks to strong *out-of-distribution generalization*. This has been additionally supported by recent work [6], which introduced the auto-encoder DT-CapsNet, outperforming routing-by-agreement (RBA) in terms of reconstruction quality and classification

accuracy. In this paper, we exploit a special routing procedure and architecture that implements an inductive bias that enforces a parts-to-whole object relationship between different layers to improve out-of-distribution generalization. It will be demonstrated experimentally that such inductive bias helps to correctly detect objects that were excluded from training and greatly improves scores when compared to the state-of-the-art CNNs. When it comes to affordances [7], [8], which in robotics are typically associated with object parts (e.g., the handle of a cup affords for *grasp*), the introduced inductive bias significantly improves the detection even on unforeseen objects. We show experimentally that such better out-of-distribution generalization results in higher affordances success rates when determining the right grasping pose for an object.

The contribution of this paper is threefold. *i)* we introduce the first capsule-based affordance detection network which enforces a part-to-whole object relationship into capsules. *ii)* we experimentally show that Capsule Networks provide comparable results to CNNs when the training and test data are similar, but more importantly, we show that the proposed approach outperforms CNNs in terms of out-of-distribution generalization. *iii)* in order to show such superiority, we introduce a newly created dataset (namely UIBK dataset) which augments the UMD dataset [9] by adding 40 RGB-D images of 7 different kitchen tools. Neither the new tool instances, nor the novel viewpoints are included in the original UMD dataset. The UIBK dataset is publicly available at [github.com/gipfelen/DTCG-Net](https://github.com/gipfelen/DTCG-Net).

After presenting the related work in section II reviews, we introduce in section III our Dynamic-Tree Capsule Graph Network (DTCG-Net), which builds on DCG-Net [2] and Scale Distance Routing (SDA) [10]. In section IV, we compare our DTCG-Net with a Capsule Network using Routing by Agreement (RBA) [3] and a state-of-the-art CNN network [11]. Section V presents an experiment where affordance detection is used to let a real robot grasp previously unseen kitchen tools, providing the success rates of our approach and the aforementioned competitor networks. Finally, in section VI, we state the conclusions and provide insights about possible improvements and further research directions.

## II. RELATED WORK

Capsule Networks [3] are an evolution of Convolutional Neural Networks (CNNs), where the main component is the *capsule*. In this context, and differently from neurons in CNNs, a capsule is a vector, representing a part of an object or an entity from a class of objects. Even though Capsule Networks are trained by backpropagation, the fact that capsules are represented by vectors, information is routed by

<sup>1</sup>Department of Computer Science, University of Innsbruck, Innsbruck, Austria [antonio.rodriguez-sanchez@uibk.ac.at](mailto:antonio.rodriguez-sanchez@uibk.ac.at)

<sup>2</sup>Department of Industrial Engineering, University of Trento, Italy.

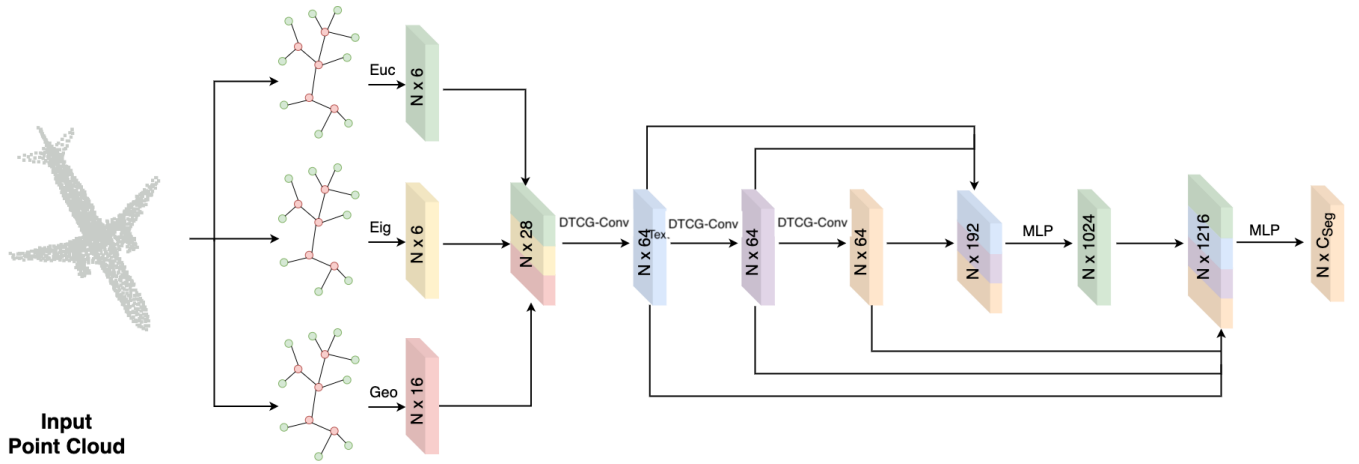


Fig. 1. Visualization of the DTCG-Net. It first extracts the eigenvalues and euclidean and geometrical features from the input point cloud. These will pass through multiple DTCG-Conv [2] modules for the prediction of the part segmentation.

an iterative algorithm. The first routing algorithm was Routing by Agreement (RBA) [3] that introduced a coupling coefficient that would represent probabilities regarding the agreement of lower layer capsules with capsules in the next capsule layer. Later, Hinton and colleagues [12] applied Expectation-Maximization in order to compute this routing. Recent routing algorithms have applied other methodologies, such as distance scaling[13], attention [14] or the use of variational bayes [15].

Capsule Networks have been widely applied, applications range from detecting actions in videos [16] to multitask learning [17], medical applications [18], [19], or 3D point clouds, the subject of this work. On the latter, one of the first works involved an auto-encoder aimed at learning 3D unstructured data [4] that showed its success in parts segmentation, object reconstruction and classification. The more recent DCG-Net [2] has been applied to these same applications, being comparable to non-capsule-based approaches such as DG-CNN [11], GS-Net [20], PointNet [21], or PointNet++ [22]. In regards to other applications of Capsule Networks in 3D point clouds, these include hand-pose estimation[23] or edge detection [24]. In relation to such tasks is the affordance estimation of parts of objects[1], [25], where Convolutional Neural Networks [22], [11], [26] can be applied to segment parts of objects that correspond to the same functionality and would then have similar affordances. We will show next that since capsules aim at representing parts of objects, it is only natural to apply Capsule Networks to such tasks.

### III. METHODS

We present here the details of our inductive bias (Sec. I) for Capsule Networks on 3D point clouds to improve out-of-distribution generalization. More precisely, with our approach, we enforce such inductive bias by generating a tree-like structure during inference. Including an inductive bias allows for *out-of-distribution generalization* [5], [6]. Affordances are very much related to object parts, as an example, handles are for *grasp* affordance. The inductive routing algorithm we

apply [13] (section III-B) enforces a tree-like structure, which is not always the case when using other routing algorithms such as RBA or EM.

In our Capsule Network, shown in Fig. 1 and named *Dynamic-Tree Capsule Network* (DTCG-Net), each capsule embodies part of an object or an object instance. We will experimentally show that enforcing this parts-to-whole object relationship improves the generalization capability of Capsule Networks.

#### A. Network Architecture

DTCG-Net’s architecture follows on DCG-Net [2], updated for a dynamic tree representation. The network uses multiple Dynamic-Tree Capsule Graph Convolutions (DTCG-Conv) modules as follows. The first DTCG-Conv layer is fed with the 3D point cloud extracting features from an eigenvalue, geometrical and euclidean nature, which are concatenated, giving rise to 28 channels as shown in Fig. 1. Such concatenated features are the input to the next DTCG-Conv layer, to which follows two additional DTCG-Conv layers. Each of these three DTCG-Conv layers are batch normalized [27] and non-linearized using leaky-ReLU [28], the slope for negative values is set to 0.2. Next, as shown in Fig. 1, through the use of skip-connections, the outputs from these three DTCG-Conv layers are accumulated into a layer that will serve as input to a fully-connected Multi-layer Perceptron (MLP) which finally provides the class label of each point that belongs to the point cloud.

#### B. Routing between capsules

In our DTCG-Net, we enforce capsules to represent a whole object or parts of it. This is of interest for affordance detection from point cloud data as capsules would represent point clouds relevant for parts representation, as opposed to methods such as CNN where the focus is on salient features leading to high-classification rates. To successfully implement this inductive bias, each capsule of the network should represent an object

**Algorithm 1** Scale-distance-agreement (SDA) [13] is the algorithm used for DTCG-Net Routing: Computes the coupling  $c_{ij}$  between the  $i$  capsules in layer  $l$  with the  $j$  capsules in layer  $l + 1$  imposing our inductive bias (see text). Input are the predictions  $\hat{u}_{j|i}$  from lower level capsule activations  $v_i$ , the number of iterations  $r$  and the layer  $l$

---

```

1: procedure SDAROUTING( $v_i, \hat{u}_{j|i}, r, l$ )
2:    $b_{ij} \leftarrow 0$ 
3:    $\hat{u}_{j|i} \leftarrow \min(\|v_i\|, \|\hat{u}_{j|i}\|) \frac{\hat{u}_{j|i}}{\|\hat{u}_{j|i}\|}$ 
4:   for  $r$  iterations do
5:      $c_{ij} \leftarrow \frac{\exp(b_{ij})}{\sum_k \exp(b_{ik})}$ 
6:      $s_j \leftarrow \sum_i c_{ij} \hat{u}_{j|i}$ 
7:      $v_j \leftarrow \frac{\|s_j\|^2}{1 + \|s_j\|^2} \frac{s_j}{\|s_j\|}$ 
8:      $t_i \leftarrow \frac{\log(0.9(J-1)) - \log(1-0.9)}{-0.5 \text{mean}_j(\|\hat{u}_{j|i} - v_j\|)}$ 
9:      $b_{ij} \leftarrow \|\hat{u}_{j|i} - v_j\| t_i$ 
10:  end for
11: end procedure

```

---

instance or one of its component parts during inference. The most usual routing algorithms do not always represent a part’s whole relationship [13]. If we are to use vector distances instead of the vector product present in routing-by-agreement (RBA), capsules represent the object part in a dynamic tree to a much higher degree as shown in 2D images [13]. We followed this idea of using vector distances in the routing algorithm in order to enforce a parts-to-whole relationships for 3D point clouds and Capsule Graph Convolutional layers. The pseudo-code is shown in Algorithm 1. Line 3 of Algorithm 1 restricts the prediction vectors to the activation of its predicting capsule. This ensures that a lower level capsule can only activate an upper level capsule when the correlated feature of this capsule is present in the current input. Line 4 represents the calculation of the coupling coefficient, which is used to calculate the output of higher level capsules in lines 5 and 6. To ensure a strong parse tree structure with a large coupling coefficient the distance is multiplied with the scale factor  $t$  to get the scaled distance agreement (line 9).

### C. Evaluation Metrics

To compare the different networks we used 2 different scores, namely the accuracy and the mean intersection over union (mIoU).

Our network gets as input a point cloud  $\mathcal{P} = \{p_i\}_{i=1}^N$  with  $N$  points and assigns to each point a class label  $l_i$  (see Sec. III-A). We compare the network’s output labels ( $l_i$ ) with the ground truth labels ( $g_i$ ) to calculate the accuracy as:

$$accuracy = \frac{\sum_{i=1}^N \delta(l_i, g_i)}{N}, \quad (1)$$

where  $\delta(x, y)$  is the Kronecker delta function. If  $x \neq y$ , then  $\delta(x, y) = 0$  and  $\delta(x, y) = 1$  if  $x = y$ . By definition, the accuracy gives us a measure of how many points have been labeled correctly and thus how good the segmentation is.

TABLE I  
AFFORDANCE (A) COLOR (C) MAPPING.

A	Grasp	Cut	Scoop	Contain	Pound	Support	Wrap Grasp
C	Blue	Orange	Green	Red	Violet	Brown	Pink

An additional metric to measure the segmentation quality is the mean intersection over union (mIoU) [11]. It is the average of all the intersections over union (IoU). These are calculated by dividing the number of correctly classified points per segmentation category ( $c$ ) by the number of points, where either the network prediction or the ground truth label has this segmentation category:

$$IoU_c = \frac{\sum_{i=1}^N \delta(g_i, c) \cdot \delta(l_i, c)}{\sum_{i=1}^N \delta(g_i, c) + \delta(l_i, c)}. \quad (2)$$

## IV. EXPERIMENTAL EVALUATION

### A. Datasets

We perform our experimental evaluation on three datasets:

- The UMD Part Affordance dataset [9] contains RGB-D images for 105 gardening, kitchen and workshop tools from different viewpoints which are segmented into 7 different affordances. We used this dataset for training and evaluation.
- The 3D AffordanceNet (AffNet) dataset [26] is composed of 23000 shapes corresponding to 23 objects. In terms of affordances, such objects were annotated with 18 visual affordance categories. Annotations are of a multi-class and multi-label nature, meaning that each individual point can have multiple affordance labels. We used the affordance class with the largest value for each point so as to be in line with the previous dataset which provides only one label per point.
- Our UIBK dataset contains 40 RGB-D images of 7 different kitchen tools (scissor, mug, knife, spoon, turner, hammer, bowl), captured with an Intel Realsense Camera D415 and converted to RGB-D images [29]. This dataset contains additional unseen viewpoints like a top view and was used to evaluate unseen object instances as well as novel viewpoints. We increased the size of the dataset adding 360 images obtained by rotating and scaling the original ones. We repeated the augmentation twice, obtaining the UIBK-20 (rotation between  $\pm 10$  deg and scaling between  $\pm 10$  cm) and the UIBK-40 (rotation between  $\pm 20$  deg and scaling between  $\pm 20$  cm) dataset. We used the UIBK, UIBK-20 and UIBK-40 datasets only for evaluation, that is, we did not use this dataset for training in order to show the generalization capabilities of DTCG-Net.

### B. Setup

RGB-D images in the considered datasets contain much background information that we remove using the ground truth labels. Since the tested neural networks require point clouds as input, we convert RGB-D images (without background) into

point clouds with the library Open3D [30]. For clarity in the evaluation, every affordance is attached a color as shown in Tab. I.

We trained the Capsule based networks, both DTCG-Net and DCG-Net, for 200 epochs. We used an adaptive Multi-StepLR learning rate [26] with an initial learning rate of  $lr = 0.0001$ , the decay rate was set to  $\gamma = 0.1$  and two milestones were defined at 75 and 125. We included in the comparison the CNN based architecture DG-CNN. Even though there are other 3D point cloud CNN architectures [31], [32], we chose DG-CNN for its popularity, its performance, and more importantly, its ability to provide object parts, which is essential for our study. For DG-CNN, we used exponential decay learning rate [33] with an initial learning rate of  $lr = 0.003$ , a decay step of 337.620 (as defined in their git repository [34]), decay rate was set to  $\gamma = 0.5$ . The batch size for all networks was 16 and all networks were trained on an Nvidia RTX 3090.

### C. Results

Results are shown in Tab. II as well as in Fig. 2. Looking at UMD, we can see that the CNN-based network DG-CNN outperforms (in terms of both accuracy and mIoU) their capsule network counterparts by around 2% (Tab. II), while these last ones, DCG-Net as well as DTCG-Net have similar results. The same holds for AffNet, where DG-CNN has again the highest scores for the mIoU as well as for the accuracy. However, in this case DTCG-Net outperforms DCG-Net with a higher accuracy of around 3%. The mIoU is nearly the same to all three networks, where DTCG-Net is very close to DG-CNN. Thus the CNN is still the go-to method to achieve the best performance when evaluating on samples from the same dataset used for training.

Figure 2 shows the affordance output for 5 different unseen tools from UIBK dataset generated by the three different networks. We also report the accuracy and mIoU in percentages below each image. The average accuracy and mIoU over the entire dataset are listed in Tab. II. It is very important to note that, while for the UMD and AffNet we divided the dataset into a training and test sets, our datasets (UIBK, UIBK-20 and UIBK-40) was only used for testing and thus was completely unseen to all the evaluated networks (DG-CNN, DCG-Net and DTCG-Net) in order to evaluate the out-of-distribution capabilities of each network. The weights from the UMD dataset were reused since it contains the exact same tools and affordances as described in Sec. IV-A. The main goal of our DTCG-Net is to learn more general object features, which would show in reaching higher scores in scenarios of newly unseen viewpoints or novel data. The left column corresponds to the DG-CNN network, the middle column to the capsule based DCG-Net with RBA as routing and the right column to our capsule based DTCG-Net with the SDA routing.

Focusing on specific objects and affordances, for example the hammer, our network is the only one that labels the head as pound (violet points in Fig. 2a). In this case, the DG-CNN network not only fails at detecting the pounding affordance, but also annotates a part of the handle with the cut (orange)

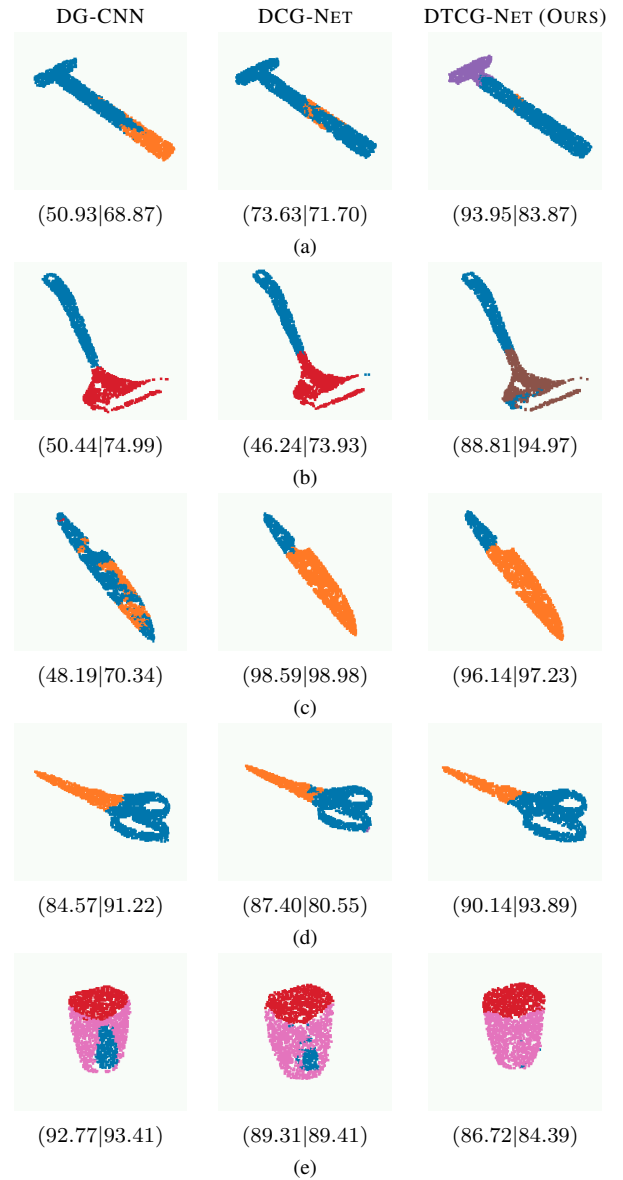


Fig. 2. Segmentation output of the different networks with unseen tools from UIBK dataset: a) hammer, b) turner, c) knife, d) scissors, and e) mug. We report (accuracy [%] | mIoU [%]) under each image.

label, achieving an accuracy of just 50.93%. DCG-Net also fails to detect the pounding part, but it achieves a higher accuracy of 73.63%. Our DTCG-Net is the most accurate (93.95%). The same can be said about the turner, where DG-CNN and DCG-Net label the bottom part as contain (red), DTCG-Net labels it as support (brown). This results in low accuracies for DG-CNN and DCG-Net (accuracies of 50.44% and 46.24% respectively), while DTCG-Net did the segmentation properly with an accuracy of 88.81%. DTCG-Net also gets similar results to DCG-Net for the knife with both networks that reasonably label grasp (blue) and cut (orange) with an accuracy of 96.14% and 98.58% respectively. On the same object, DG-CNN performs poorly (accuracy of 48.19%) mixing up grasp and cut points. For the

TABLE II  
ACCURACY AND mIoU FOR THE THREE DIFFERENT NETWORKS ON THE AFFNET [26], THE UMD [9], AND OUR DATASETS.

TEST DATASET	TRAIN DATASET	DG-CNN		DCG-NET		DTCG-NET	
		ACCURACY [%]	mIoU [%]	ACCURACY [%]	mIoU [%]	ACCURACY [%]	mIoU [%]
UMD	UMD	97.46	98.09	95.24	96.30	95.17	96.18
AFFNET	AFFNET	67.80	89.94	61.78	88.65	64.78	89.24
UIBK	UMD	72.12	84.52	75.48	84.41	76.93	85.84
UIBK-20	UMD	69.31	82.09	70.28	81.49	71.42	82.41
UIBK-40	UMD	59.42	75.98	67.81	73.34	65.59	78.71

scissors (Fig. 2d), all three networks performed similarly well (accuracy of 84.57%, 87.40% and 90.14% for DG-CNN, DCG-Net and DTCCG-Net respectively). This is probably due to the fact that we could incorporate less variability to this object and the views obtained were similar to the ones present in the UMD dataset [9]. DTCCG-Net performs well on all the objects, apart from the mug (accuracy of 86.72%) where it almost missed the handle (Fig. 2e). On the same object, DG-CNN is the most accurate followed by DCG-Net (accuracy of 92.77% and 89.31% respectively). This behavior is probably due to the inductive bias enforced in DTCCG-Net that tends to segment the object into fewer but larger segments. While this behavior provides a clear advantage for object segmentation—thanks to a more clear separation between segments—leading to better affordance labeling in most cases, it has the downside of neglecting parts that are too small. To summarize, Fig. 2 qualitatively shows several examples where our approach (DTCCG-Net) clearly outperforms DCG-Net and DG-CNN (Fig. 2a to 2c), provides similar results (Fig. 2d), and slightly worse values (Fig. 2e). For a more rigorous analysis, we show in Tab. II the accuracy and the mIoU (Sec. III-C) for UMD, AffNet, and UIBK (-20, -40) datasets evaluated on all three networks.

Analyzing the results shown in Tab. II we notice that, if we are to evaluate the three networks with previously not seen data (our three UIBK datasets), DG-CNN provides now the worst results, while the capsule-based networks hold stronger. For the UIBK dataset (40 images), DTCCG-Net shows the best accuracy (76.93%) and mIoU (85.84%), compared with DCG-Net (accuracy of 75.48% and mIoU 84.41%) and DG-CNN (accuracy of 72.12% and mIoU 84.51%). While the accuracy of the DTCCG-Net drops by around 18%, the accuracy of DG-CNN drops by around 25%. The same holds true for the mIoU where the DG-CNN drops by around 4% more than the DTCCG-Net. Finally, all the approaches have similar standard deviation ranges on our dataset (DG-CNN ranges from 27% to 34%, DCG-Net ranges from 28% to 30%, and DTCCG-Net ranges from 23% to 30%). Results on the augmented datasets UIBK-20 and UIBK-40 (400 images each) tend to confirm that capsule-based methods outperform the CNN-based ones, especially in terms of accuracy.

These results show that the capsule-based networks seem to improve out-of-distribution generalization so that they can be used on unseen object classes. In specific applications, such

as the grasping of unknown objects, capsule-based networks could be of great interest since they tend to outperform current state-of-the-art CNN-based networks (Sec. I).

We believe this is because capsule networks encode better the objects based on their parts and uses the spatial information as well as computing probabilities of an object being present thanks to the nature of the capsule routing [3]. On the other hand, the CNN only tries to locate discriminating features anywhere in the data without taking into account spatial location or part-based object representations.

## V. AFFORDANCE-BASED GRASPING

To show the effectiveness of our affordance detection network in a real-world scenario, we conducted a grasping experiment with multiple objects and a robot. The goal is to detect the *Grasp* affordance on the observed object and then grasp it. To this end, we used a Franka Emika Panda manipulator mounting an Intel RealSense D415 camera at its end-effector (Fig. 3). As in Sec. IV, we compare the results obtained with DG-CNN, DCG-Net, and DTCCG-Net.

### A. Processing pipeline

The pipeline used to retrieve a grasping pose from sensory data consists of the following steps.

- 1) *Capturing the image.* We directly capture an RGB-D image from the Intel Realsense Depth Camera D415.
- 2) *Background removal.* The background is removed from the RGB-D image by placing the objects on a blue surface and removing the biggest blue contour within the image using OpenCV [35]. We have also tested the plane detection approach proposed by Zhou et al. [30], but results were not reliable because flat objects were often misinterpreted as being part of the plane.
- 3) *Conversion to point cloud.* We convert the area of interest to a point cloud with the library Open3D [30] and reduce the amount of points to 2048.
- 4) *Prediction of the network.* We feed the point cloud to the networks in order to get an affordance prediction for the observed object.
- 5) *Finding the biggest cluster of type grasp.* To reduce noise and outlier effects, we select the biggest cluster of *Grasp* points.
- 6) *Grasping pose estimation.* Grasping position is computed as the mean of the points in the *Grasp* cluster.

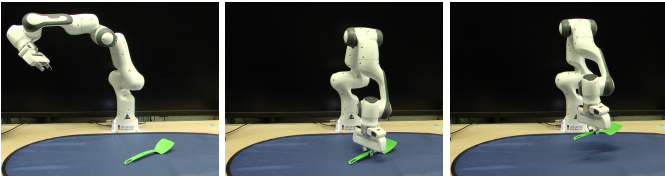


Fig. 3. The robot successfully grasps the turner.

For the orientation, we perform a principal component analysis and get 3 axes forming a rotation matrix.

- 7) *Grasping the object.* We use Cartesian impedance control [36] to reach the object to grasp. Grasping position is directly fed to the robot. For the orientation, we compute the rotation needed to make the gripper fingers orthogonal to the major axis (longest dimension) of the object. This is obtained by computing the angle between the gripper  $x$ -axis and the first principal component computed in step 6). With the gripper closed, the robot lifts the object 10 cm and we visually determine if it is firmly grasped (Fig. 3).

### B. Results

We used 6 different objects (spoon, fork, hammer, knife, cup, and turner) which we tried to grasp at 4 different orientations. These objects are part of the UIBK dataset, but captured from unseen viewpoints. Each grasping experiment was performed twice to evaluate repeatability. Overall, the robot has to perform 48 grasps for each of the 3 networks. For each run, we checked if the grasp was successful, measured the distance from the ideal grasping point and the deviation (in degrees) for the rotation between the robot and the grasping part. The distance to the grasping point (centroid) is of importance in antipodal grasping because grasping far from the centroid may easily cause the object to tilt. Keeping the correct orientation wrt the grasping part is also important to prevent undesired collisions with the object. We defined a grasp attempt as successful if the object was grasped at a grasping point and the robot was able to pick it up. The grasping point was defined by hand for each object, by taking the geometric center of the biggest grasping part.

Table III shows the average results over all runs for each network. The success rates denote how many grasp attempts were successful. The distance as well as the angle gives the average distance over all runs for each algorithm shows that DTCG-Net outperforms both DCG-Net and DG-CNN. The robot successfully performed 42 out of 48 grasps with DTCG-Net, 34 out of 48 with DG-CNN, and 32 out of 48 with DCG-Net. In other words, the success rate with DTCG-Net was 16.7% higher when compared to the best baseline approach. Using DTCG-Net, the average distance between actual and ideal grasping points decreased by 13.6% (0.3 cm) and the average grasping angle deviation decreased by 46.9% (9.2 deg) compared to DG-CNN (the second best network).

The results from this experiment coincide with those shown in Sec. IV regarding novel objects and viewpoints. We assume

TABLE III  
RESULTS OF THE AFFORDANCE-BASED GRASPING EXPERIMENTS.

NETWORK	SUCCESS RATE [%]	DISTANCE [CM]	ANGLE [DEG]
DG-CNN	70.8	2.2	19.6
DCG-NET	66.7	2.7	23.3
DTCG-NET	87.5	1.9	10.4

that, due to the better affordance detection of the DTCG-Net when confronted with unseen object instances from new viewpoints, the robot is able to perform its grasping task with a higher success rate and with lower error values.

### VI. CONCLUSIONS

In this work, we have presented the Dynamic-Tree Capsule Graph Network (DTCG-Net) for affordance detection. Different capsule networks were developed for processing 3D point clouds to ensure equivariant representations of capsule vectors w.r.t. rotations, translations, and permutations of inputs [2], [37]. To the best of our knowledge, we are the first that not only use capsule layers to produce equivariant vectors but also, the proposed DTCG-Net additionally leverages a particular routing algorithm (SDA) to enforce a part-to-whole object inductive bias on the capsules. As demonstrated in the experimental section, this inductive bias improves out-of-distribution generalization capabilities which are very well suited for affordance detection even on unseen object instances.

We have shown qualitatively that our DTCG-Net capsule network outperforms DCG-Net in terms of accuracy and mIoU. The current state-of-the-art CNN based network DG-CNN still outperforms capsule-based networks at 3D point-cloud classification, including our own DTCG-Net, even if it is by a small margin. However, our DTCG-Net outperforms not only DCG-Net, but also such state-of-the-art CNN when the object instances or views were not presented at training – which are extremely important in robotic tasks – due to DTCG-Net’s better out-of-distribution generalization capabilities. We additionally evaluated affordance detection with those unseen object instances to show how the aforementioned neural networks can handle unseen objects and new viewpoints and provided a task of affordance detection and grasping. Here, the robot was faced with the grasping of new unseen object instances from new viewpoints. DTCG-Net performed by far the best with the highest success rate of object grasping, the lowest average distance to the ideal grasp point as well as lowest average grasping angle deviation, which shows the superiority of our network in robotic tasks. Behind the success of DTCG-Net over not only DCG-Net, but also the state-of-the-art DTCG-Net at these affordances tasks is the inductive bias implemented through SDA routing. This inductive bias allows to detect objects not used during training since the focus is not so much on the highest-performance feature extraction (as in the CNN methods like DG-CNN), but on a meaningful feature extraction for parts representing objects which can be

done thanks to Capsule Networks routing algorithms such as SDA, which is specifically designed to build a tree-like structure.

Future work would include extending DTCG-Net to provide a direct pose estimation for each detected affordance to avoid the heuristic definition of the grasping orientation. SDA's routing could be also updated to better handle small object parts and evaluate other routing algorithms like recent Variational Bayes [38] or dot-product attention routing [39].

## REFERENCES

- [1] T.-T. Do, A. Nguyen, and I. Reid, "Affordancenet: An end-to-end deep learning approach for object affordance detection," in *2018 IEEE international conference on robotics and automation (ICRA)*. IEEE, 2018, pp. 5882–5889.
- [2] D. Bazazian and D. Nahata, "Dcg-net: Dynamic capsule graph convolutional network for point clouds," *IEEE Access*, vol. 8, pp. 188056–188067, 2020.
- [3] S. Sabour, N. Frosst, and G. E. Hinton, "Dynamic routing between capsules," *arXiv preprint arXiv:1710.09829*, vol. abs/1710.09829, 2017. [Online]. Available: <http://arxiv.org/abs/1710.09829>
- [4] Y. Zhao, T. Birdal, H. Deng, and F. Tombari, "3d point-capsule networks," in *Proceedings of the IEEE/CVF Conference on Computer Vision and Pattern Recognition*, 2019, pp. 1009–1018.
- [5] A. Goyal and Y. Bengio, "Inductive biases for deep learning of higher-level cognition," *arXiv preprint arXiv:2011.15091*, 2020.
- [6] C. Engelhardt, J. Mittelberger, D. Peer, S. Stabinger, and A. Rodríguez-Sánchez, "Improving 3d point cloud reconstruction with dynamic tree-structured capsules," in *Proceedings of the IEEE/CVF Winter Conference on Applications of Computer Vision*, 2022 (under review).
- [7] H. Min, R. Luo, J. Zhu, S. Bi, *et al.*, "Affordance research in developmental robotics: A survey," *IEEE Transactions on Cognitive and Developmental Systems*, vol. 8, no. 4, pp. 237–255, 2016.
- [8] P. Zech, S. Haller, S. Rezapour Lakani, B. Ridge, E. Ugur, and J. Piater, "Computational models of affordance in robotics: a taxonomy and systematic classification," *Adaptive Behavior*, vol. 25, no. 5, pp. 235–271, 2017.
- [9] A. Myers, C. L. Teo, C. Fermüller, and Y. Aloimonos, "Affordance detection of tool parts from geometric features," in *ICRA*, 2015.
- [10] D. Peer, S. Stabinger, and A. Rodríguez-Sánchez, "Training deep capsule networks," *arXiv preprint arXiv:1812.09707*, 2018.
- [11] Y. Wang, Y. Sun, Z. Liu, S. E. Sarma, M. M. Bronstein, and J. M. Solomon, "Dynamic graph cnn for learning on point clouds," *Acm Transactions On Graphics (tog)*, vol. 38, no. 5, pp. 1–12, 2019.
- [12] G. E. Hinton, S. Sabour, and N. Frosst, "Matrix capsules with EM routing," in *International Conference on Learning Representations*, 2018.
- [13] D. Peer, S. Stabinger, and A. Rodríguez-Sánchez, "Increasing the adversarial robustness and explainability of capsule networks with  $\gamma$ -capsules," *arXiv preprint arXiv:1812.09707*, 2018.
- [14] Y.-H. H. Tsai, N. Srivastava, H. Goh, and R. Salakhutdinov, "Capsules with inverted dot-product attention routing," in *International Conference on Learning Representations*, 2019.
- [15] F. D. S. Ribeiro, G. Leontidis, and S. Kollias, "Capsule routing via variational bayes," in *Proceedings of the AAAI Conference on Artificial Intelligence*, vol. 34, no. 04, 2020, pp. 3749–3756.
- [16] K. Duarte, Y. S. Rawat, and M. Shah, "Videocapsulenet: A simplified network for action detection," *arXiv preprint arXiv:1805.08162*, vol. abs/1805.08162, 2018. [Online]. Available: <http://arxiv.org/abs/1805.08162>
- [17] L. Xiao, H. Zhang, W. Chen, Y. Wang, and Y. Jin, "Mcapsnet: Capsule network for text with multi-task learning," in *Proceedings of the 2018 conference on empirical methods in natural language processing*, 2018, pp. 4565–4574.
- [18] D. Zhang, B. Wang, G. Wang, Q. Zhang, J. Zhang, J. Han, and Z. You, "Onfocus detection: Identifying individual-camera eye contact from unconstrained images," *arXiv preprint arXiv:2103.15307*, 2021.
- [19] P. Afshar, S. Heidarian, F. Naderkhani, A. Oikonomou, K. N. Plataniotis, and A. Mohammadi, "Covid-caps: A capsule network-based framework for identification of covid-19 cases from x-ray images," *Pattern Recognition Letters*, vol. 138, pp. 638–643, 2020.
- [20] M. Xu, Z. Zhou, and Y. Qiao, "Geometry sharing network for 3d point cloud classification and segmentation," in *Proceedings of the AAAI Conference on Artificial Intelligence*, vol. 34, no. 07, 2020, pp. 12500–12507.
- [21] C. R. Qi, H. Su, K. Mo, and L. J. Guibas, "Pointnet: Deep learning on point sets for 3d classification and segmentation," in *Proceedings of the IEEE conference on computer vision and pattern recognition*, 2017, pp. 652–660.
- [22] C. R. Qi, L. Yi, H. Su, and L. J. Guibas, "Pointnet++: Deep hierarchical feature learning on point sets in a metric space," *arXiv preprint arXiv:1706.02413*, 2017.
- [23] Y. Wu, S. Ma, D. Zhang, and J. Sun, "3d capsule hand pose estimation network based on structural relationship information," *Symmetry*, vol. 12, no. 10, 2020. [Online]. Available: <https://www.mdpi.com/2073-8994/12/10/1636>
- [24] D. Bazazian and M. E. Parés, "Edc-net: Edge detection capsule network for 3d point clouds," *Applied Sciences*, vol. 11, no. 4, p. 1833, Feb. 2021. [Online]. Available: <https://doi.org/10.3390/app11041833>
- [25] F.-J. Chu, R. Xu, C. Tang, and P. A. Vela, "Recognizing object affordances to support scene reasoning for manipulation tasks," *arXiv preprint arXiv:1909.05770*, 2019.
- [26] S. Deng, X. Xu, C. Wu, K. Chen, and K. Jia, "3d affordancenet: A benchmark for visual object affordance understanding," 2021.
- [27] S. Ioffe and C. Szegedy, "Batch normalization: Accelerating deep network training by reducing internal covariate shift," *CoRR*, vol. abs/1502.03167, 2015. [Online]. Available: <http://arxiv.org/abs/1502.03167>
- [28] B. Xu, N. Wang, T. Chen, and M. Li, "Empirical evaluation of rectified activations in convolutional network," *CoRR*, vol. abs/1505.00853, 2015. [Online]. Available: <http://arxiv.org/abs/1505.00853>
- [29] S. Dorodnicov, D. Hirshberg, M. Horn, R. Lopez, and I. Carpis, "Intel® realsense™ sdk." [Online]. Available: <https://github.com/IntelRealSense/librealsense>
- [30] Q.-Y. Zhou, J. Park, and V. Koltun, "Open3D: A modern library for 3D data processing," *arXiv:1801.09847*, 2018.
- [31] H. Thomas, C. R. Qi, J.-E. Deschaud, B. Marcotegui, F. Goulette, and L. J. Guibas, "Kpconv: Flexible and deformable convolution for point clouds," in *Proceedings of the IEEE/CVF international conference on computer vision*, 2019, pp. 6411–6420.
- [32] H. Chen, S. Liu, W. Chen, H. Li, and R. Hill, "Equivariant point network for 3d point cloud analysis," in *Proceedings of the IEEE/CVF Conference on Computer Vision and Pattern Recognition*, 2021, pp. 14514–14523.
- [33] A. Paszke, S. Gross, F. Massa, A. Lerer, J. Bradbury, G. Chanan, T. Killeen, Z. Lin, N. Gimelshein, L. Antiga, A. Desmaison, A. Kopf, E. Yang, Z. DeVito, M. Raison, A. Tejani, S. Chilamkurthy, B. Steiner, L. Fang, J. Bai, and S. Chintala, "Pytorch: An imperative style, high-performance deep learning library," in *Advances in Neural Information Processing Systems 32*, H. Wallach, H. Larochelle, A. Beygelzimer, F. d'Alché Buc, E. Fox, and R. Garnett, Eds. Curran Associates, Inc., 2019, pp. 8024–8035.
- [34] Y. Wang, Y. Sun, Z. Liu, S. E. Sarma, M. M. Bronstein, and J. M. Solomon, "Dynamic graph cnn for learning on point clouds git repository." [Online]. Available: <https://github.com/WangYueFu/dgcn>
- [35] G. Bradski, "The OpenCV Library," *Dr. Dobbs' Journal of Software Tools*, 2000.
- [36] C. Ott, *Cartesian Impedance Control: The Rigid Body Case*. Berlin, Heidelberg: Springer Berlin Heidelberg, 2008, pp. 29–44.
- [37] Y. Zhao, T. Birdal, J. E. Lenssen, E. Menegatti, L. Guibas, and F. Tombari, "Quaternion equivariant capsule networks for 3d point clouds," in *European Conference on Computer Vision*. Springer, 2020, pp. 1–19.
- [38] F. D. S. Ribeiro, G. Leontidis, and S. D. Kollias, "Capsule routing via variational bayes," *CoRR*, vol. abs/1905.11455, 2019. [Online]. Available: <http://arxiv.org/abs/1905.11455>
- [39] Y.-H. H. Tsai, N. Srivastava, H. Goh, and R. Salakhutdinov, "Capsules with inverted dot-product attention routing," 2020. [Online]. Available: <https://arxiv.org/pdf/2002.04764.pdf>